

## Supporting Information

### Photocatalytic hydrogen evolution by Cu(II) complexes

Junfei Wang,<sup>a,b</sup> Chao Li,<sup>a</sup> Qianxiong Zhou,<sup>a</sup> Weibo Wang,<sup>a</sup> Yuanjun Hou,<sup>\* a</sup> Baowen Zhang,<sup>a</sup>  
Xuesong Wang<sup>\* a</sup>

<sup>a</sup> Key Laboratory of Photochemical Conversion and Optoelectronic Materials, Technical Institute  
of Physics and Chemistry, Chinese Academy of Sciences, Beijing 100190, P. R. China

<sup>b</sup> Graduate School of Chinese Academy of Sciences, Beijing 100049, P. R. China

#### Table of Contents

1. Synthesis and characterization.
2. **Figure S1:** ESI-MS spectra of **1** and **2**.
3. **Figure S2:** UV-visible absorption spectra of **1** and **2**.
4. **Figure S3:** <sup>1</sup>H NMR spectra of **1** and **2**.
5. **Figure S4-S8:** Optimization of the photocatalytic H<sub>2</sub> production conditions.
6. **Figure S9:** Cyclic voltammograms of **1**, **2**, TMPA, Cl-TMPA, Zn-TMPA and Zn-Cl-TMPA.
7. **Figure S10:** Cyclic voltammograms of 6-chloro-2-picoline.
8. **Figure S11:** Cyclic voltammograms of acetic acid and **2** in CH<sub>3</sub>CN.
9. **Figure S12-13:** Cyclic voltammograms of **1** and **2** at different scan rates.
10. **Figure S14:** Cyclic voltammograms of **2** with or without the presence of acetic acid.
11. **Figure S15:** Absorption spectra of **1** and **2** before and after electrolysis.
12. **Figure S16-18:** Luminescence quenching of [Ir(ppy)<sub>2</sub>(dtbpy)]Cl by **1**, **2** and TEA.
13. **Table S1.** Crystal data and structure refinement for **2**.
14. **Table S2.** Selected bond lengths (Å) and angles (deg) for **2**.

**Materials.** Copper(II) chloride dihydrate, di-(2-picoly)amine, sodium triacetoxyborohydride, 6-chloro-2-pyridinecarboxaldehyde, 2-pyridinecarboxaldehyde and 6-chloro-2-picoline were purchased from Adamas. Triethylamine (TEA) and tetrabutylammonium hexafluorophosphate were obtained from Alfa. All solvents were of analytical purity and used without further treatment. Distilled water was used in all experiments.

**Instrumentation.** <sup>1</sup>H NMR spectra were obtained on a Bruker DMX-400 MHz spectrophotometer. HR-MS were taken on a Bruker APEX IV (7.0T) FT\_MS. Elemental analysis was performed on a FLASH EA1112 elemental analyzer. UV-Vis absorption spectra were recorded on a Shimadzu UV-2450 spectrophotometer. Fluorescence emission spectra were run on a Hitachi F-4600 fluorescence spectrophotometer.

**Photocatalytic H<sub>2</sub> evolution.** A 10 mL of CH<sub>3</sub>CN/H<sub>2</sub>O (9:1, v/v) solution containing 0.2 mM [Ir(ppy)<sub>2</sub>(dtbpy)]Cl, 1 μM copper complex, and 0.45 M TEA was put into a 40 mL glass vial equipped with a rubber-septum-sealed outlet. After bubbling with argon for 25 min, 3 mL of gas in the vial was removed by a syringe and 3 mL of methane was injected into the reaction vessel to serve as the internal standard for H<sub>2</sub> quantification. Then the vial was irradiated with visible light, which was obtained from a 1000 W solar simulator (Oriel 91192) using a 400-nm-long pass glass filter and a distilled water pool to cut off the UV and IR light, respectively. The production of H<sub>2</sub> was monitored and quantified by gas chromatography on a Shimadzu GC-2014 (thermal conductivity detector, 5 Å molecular sieve, 30 m × 0.53 mm column, N<sub>2</sub> gas carrier). The photocatalytic H<sub>2</sub> evolution quantum yields (QE) of the examined systems were measured according to the following equation, where the incident light intensity was measured by a 70260 radiation power meter with a thermopile probe (Oriel Instruments).

$$\text{QE} = \frac{\text{number of evolved H}_2 \text{ molecules} \times 2}{\text{number of incident photons}} \times 100\%$$

**Electrochemistry.** The redox potentials were measured on an EG&G model 283 potentiostat/galvanostat in a three-electrode cell with a glassy carbon working electrode, a platinum-plate counter electrode, and a SCE (saturated calomel electrode) reference electrode. Cyclic voltammetry was conducted at a scan rate of 100 mV s<sup>-1</sup> in an argon-saturated anhydrous CH<sub>3</sub>CN containing 0.1 M *n*-Bu<sub>4</sub>NPF<sub>6</sub> as the supporting electrolyte.

**Luminescence quenching experiments.** All quenching experiments were done by adding calibrated amounts of quencher into the [Ir(ppy)<sub>2</sub>(dtbpy)]Cl solution at room temperature. The [Ir(ppy)<sub>2</sub>(dtbpy)]Cl concentration was fixed at 10 μM in CH<sub>3</sub>CN/H<sub>2</sub>O (9:1, v/v). The solutions were degassed with argon for 25 min. Steady-state luminescence spectra were then collected for each sample. The relative emission intensity of the chromophore in the absence and presence of a

quencher was used to calculate the bimolecular quenching rate constant  $k_q$  by the Stern-Volmer equation (eq. 1), where  $I_0$  and  $I$  are the integrated emission intensity of the Ir-based photosensitizer in the absence or presence of a quencher, and  $\tau_0$  ( $0.557 \mu\text{s}^{-1}$ ) is the triplet excited state lifetime of the Ir-based photosensitizer without the presence of quencher.

$$I_0/I = 1 + k_q\tau_0[Q] \quad \text{----- (1)}$$

## Synthesis<sup>2</sup>

**Tris(2-pyridyl)methylamine (TMPA).** 2-pyridinecarboxaldehyde (0.58 g, 5.38 mmol) and di-(2-picolyl) amine (0.98 g, 4.91 mmol) were dissolved in 20 mL of 1,2-dichloroethane in a 50 mL two-neck-flask and sodium triacetoxyborohydride (1.66 g, 7.85 mmol) was added into the solution. The mixture was stirred for 2 days under Ar. The solvent was removed by high vacuum rotary evaporation. The resulting crude product was dissolved in 20 mL of  $\text{CH}_2\text{Cl}_2$ , washed twice with saturated  $\text{Na}_2\text{CO}_3$  solution. After drying over  $\text{MgSO}_4$  and filtration, the solvent was removed by rotary evaporation. The resulting yellow oil was purified by column chromatography on alumina (ethylacetate as eluent) to yield a yellowish solid.  $^1\text{H NMR}$  (400 MHz,  $\text{CDCl}_3$ ):  $\delta$  8.54 (d,  $J = 4.8$  Hz, 3H), 7.68–7.59 (m, 6H), 7.16–7.13 (m, 3H), 3.92 (s, 6H).

**1-(6-Chloropyridin-2-yl)-N, N-bis(pyridin-2-ylmethyl)methanamine (Cl-TMPA).** Following the synthetic method for TMPA and using 6-chloro-2-pyridinecarboxaldehyde (0.76 g, 5.38 mmol) instead of 2-pyridinecarboxaldehyde, Cl-TMPA was prepared as a yellowish solid.  $^1\text{H NMR}$  (400 MHz,  $\text{CDCl}_3$ ):  $\delta$  8.55 (d,  $J = 4.4$  Hz, 2H), 7.64–7.54 (m, 6H), 7.18–7.14 (m, 3H), 3.90 (s, 6H).

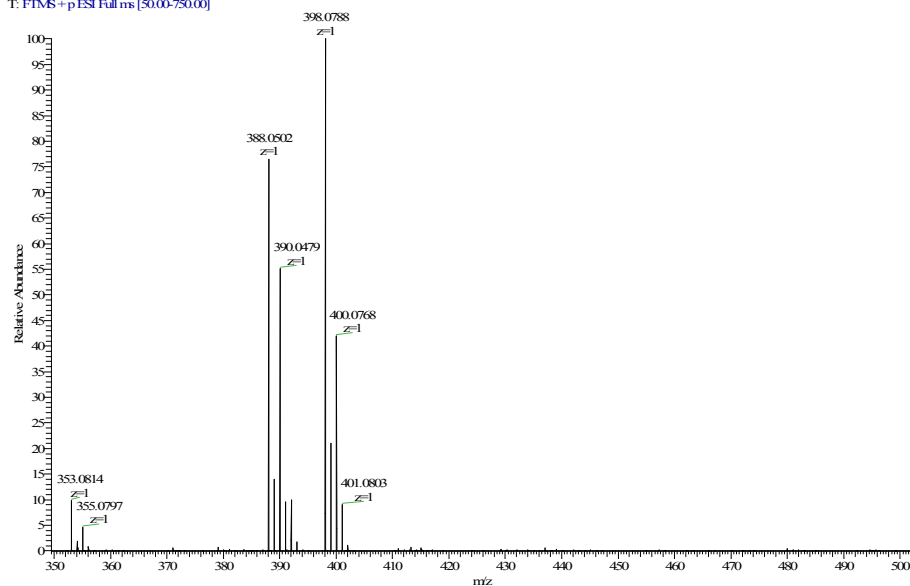
**[Cu(TMPA)Cl]Cl (1).** In a 50 mL Schlenk flask, 64.7 mg (0.2 mmol) of TMPA was dissolved in 5 mL dry acetone. 34.1 mg (0.2 mmol) of  $\text{CuCl}_2 \cdot 2\text{H}_2\text{O}$  was dissolved in 5 mL dry acetone and then added to TMPA solution. After stirring for 10 min at room temperature, the complex was precipitated as blue solid upon addition of diethyl ether (50 mL). The supernatant was decanted and the resulting blue solid was washed twice with diethyl ether and dried under vacuum to afford 79 mg of Cu(II) complex. Single crystals were obtained by vapor diffusion of diethyl ether into a solution of the complex in  $\text{CH}_3\text{CN}$ . HR ESI-MS (Figure S1):  $m/z = 388.0499$  ( $[\text{Cu}(\text{TMPA})\text{Cl}]^+$ ), 398.0785 ( $[\text{Cu}(\text{TMPA}) + \text{COOH}]^+$ ). The latter signal resulted from the interaction of the Cu complex with  $\text{HCOOH}$  which was present in the matrix. Elemental Analysis: Anal. calcd for  $\text{C}_{18}\text{H}_{18}\text{N}_4\text{Cl}_2\text{Cu}$ : C, 50.89; H, 4.27; N, 13.19. Found: C, 50.77; H, 4.37; N, 13.20. UV-visible absorption (Figure S2):  $\lambda_{\text{max}}$  255 nm ( $\epsilon = 13980 \text{ M}^{-1} \text{ cm}^{-1}$ ), 291 nm ( $3040 \text{ M}^{-1} \text{ cm}^{-1}$ ), 760 nm ( $273 \text{ M}^{-1} \text{ cm}^{-1}$ ). The UV bands may be ascribed to the ligand  $\pi \rightarrow \pi^*$  transitions and the NIR band to the  $\text{Cu}^{\text{II}}$  d-d transition.<sup>3</sup>  $^1\text{H NMR}$  (400 MHz,  $\text{CD}_3\text{CN}$ , Figure S3):  $\delta$  30 (broad), 10.5 (sharp). The  $^1\text{H NMR}$  spectrum of **1** is very similar to that of  $[\text{Cu}(\text{TMPA})\text{CH}_3\text{CN}](\text{ClO}_4)_2$ .<sup>4</sup>

**[Cu(Cl-TMPA)Cl<sub>2</sub>] (2).** Following the synthetic method for **1** and using Cl-TMPA instead of TMPA, **2** was prepared as a blue solid and its single crystals suitable for X-ray diffraction analysis

were obtained by vapor diffusion of diethyl ether into a solution of the complex in  $\text{CH}_3\text{CN}$ . HR ESI-MS (Figure S1):  $m/z = 387.0421$  ( $[\text{Cu}(\text{Cl-TMPA})]^+$ ),  $432.0398$  ( $[\text{Cu}(\text{Cl-TMPA}) + \text{COOH}]^+$ ). Elemental Analysis: Anal. calcd for  $\text{C}_{18}\text{H}_{17}\text{N}_4\text{Cl}_3\text{Cu}$ : C, 47.07; H, 3.73; N, 12.20. Found: C, 47.23; H, 3.77; N, 12.38. UV-visible absorption (Figure S2):  $\lambda_{\text{max}}$  259 nm ( $14140 \text{ M}^{-1} \text{ cm}^{-1}$ ), 291 nm ( $2740 \text{ M}^{-1} \text{ cm}^{-1}$ ), 728 nm ( $160 \text{ M}^{-1} \text{ cm}^{-1}$ ). The UV bands may be ascribed to the ligand  $\pi \rightarrow \pi^*$  transitions and the NIR band to the  $\text{Cu}^{\text{II}}$  d-d transition.<sup>2</sup>  $^1\text{H}$  NMR (400 MHz,  $\text{CD}_3\text{CN}$ , Figure S3):  $\delta$  in ppm 10.34 (sharp), 9.613 (sharp), 7.926 (sharp).

**a**

Wangjunfei-27 #9 RT: 0.10 AV: 1 NL: 7.06E7  
T: FTMS+pESI Full ms [50.00-750.00]



**b**

Wangjunfei-28 #9 RT: 0.10 AV: 1 NL: 1.25E7  
T: FTMS+pESI Full ms [50.00-750.00]

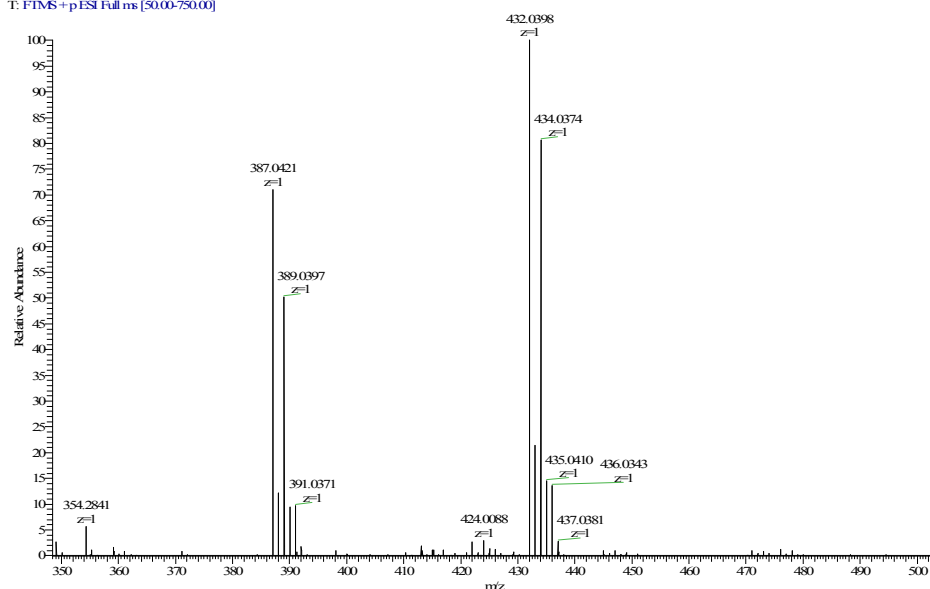


**Figure S1.** ESI-MS spectra of **1** (a) and **2** (b).

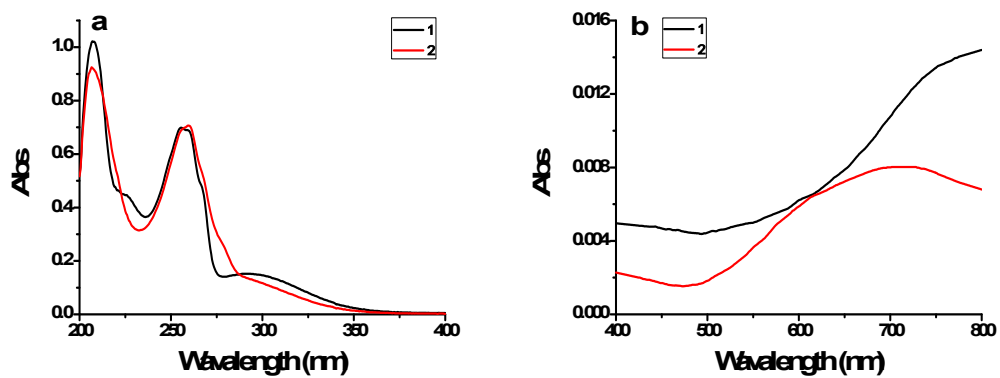


**Figure S2.** UV-visible absorption spectra of **1** and **2** (0.05 mM) within 200-400 nm (a) and 400-800 nm (b) in CH<sub>3</sub>CN/H<sub>2</sub>O (9:1, v/v).

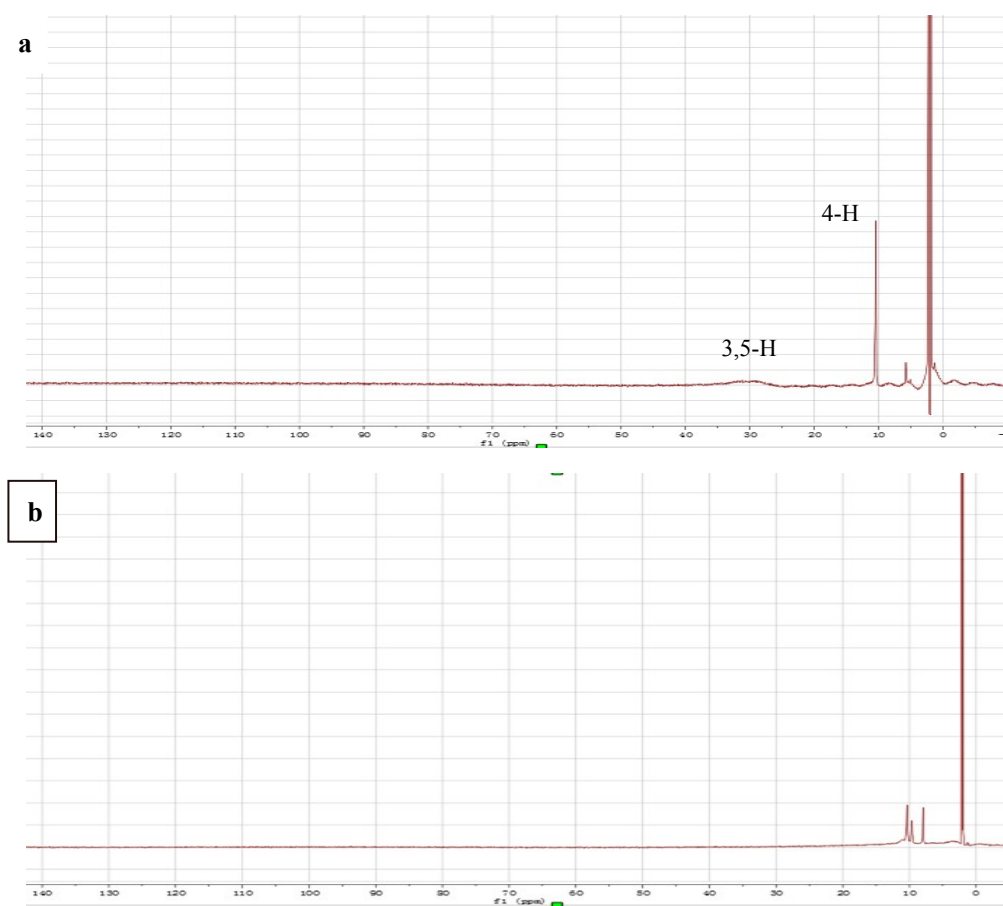


**Figure S3.** <sup>1</sup>H NMR spectra of **1** (a) and **2** (b) in CD<sub>3</sub>CN.

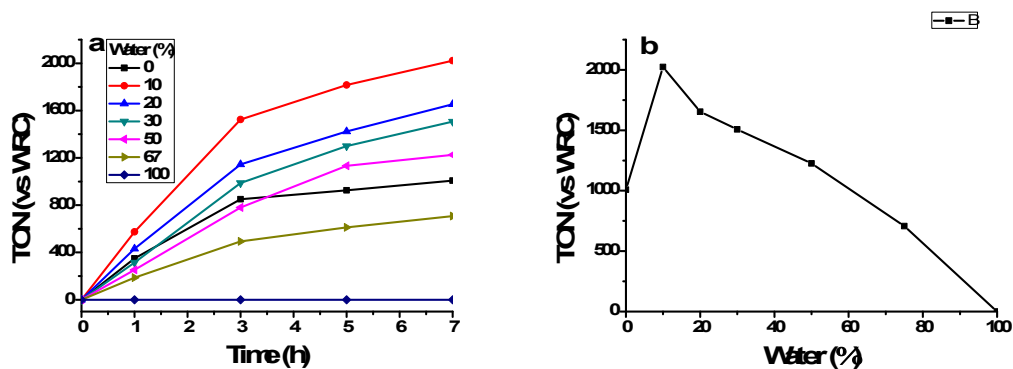


**Figure S4.** (a) Photocatalytic H<sub>2</sub> production profiles of the AP systems containing 0.1 mM [Ir(ppy)<sub>2</sub>(dtbpy)]Cl, 0.01 mM **1**, 0.6 M TEA in CH<sub>3</sub>CN/H<sub>2</sub>O of varied compositions. (b) H<sub>2</sub> production amounts of the AP systems after 7 h irradiation.

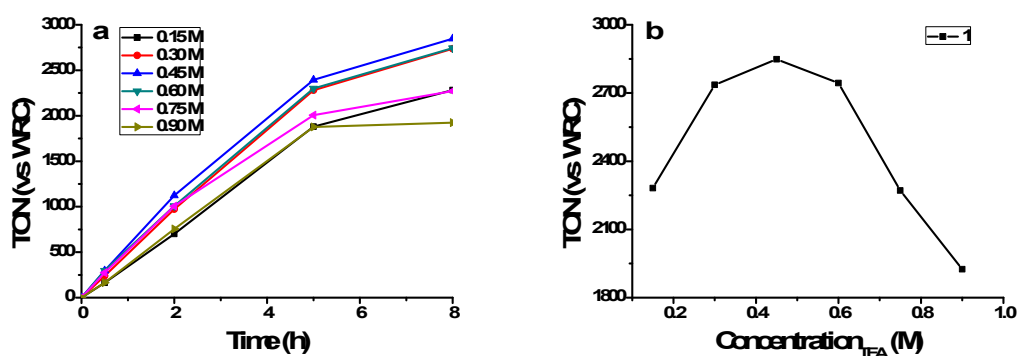


**Figure S5.** (a) Photocatalytic H<sub>2</sub> production profiles of the AP systems containing 0.1 mM [Ir(ppy)<sub>2</sub>(dtbpy)]Cl, 0.01 mM **1**, and varied concentrations of TEA in CH<sub>3</sub>CN/H<sub>2</sub>O (9:1). (b) H<sub>2</sub> production amounts of the AP systems after 8 h irradiation.

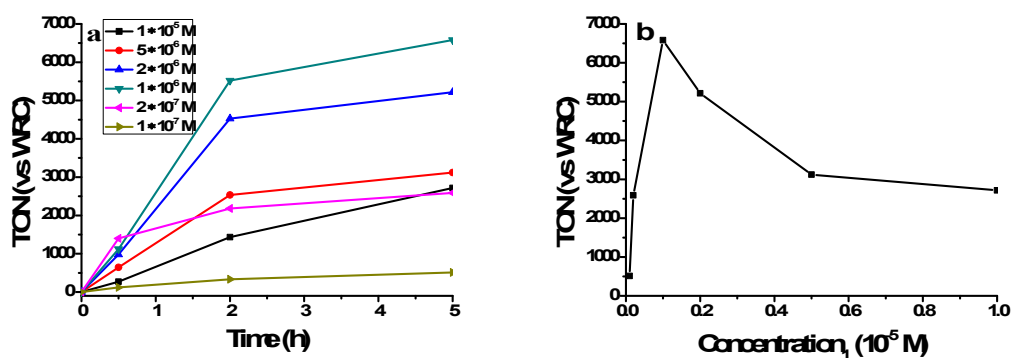


**Figure S6.** (a) Photocatalytic H<sub>2</sub> production profiles of the AP systems containing 0.1 mM [Ir(ppy)<sub>2</sub>(dtbpy)]Cl, 0.45 M TEA, and varied concentrations of **1** in CH<sub>3</sub>CN/H<sub>2</sub>O (9:1). (b) H<sub>2</sub> production amounts of the AP systems after 5 h irradiation.

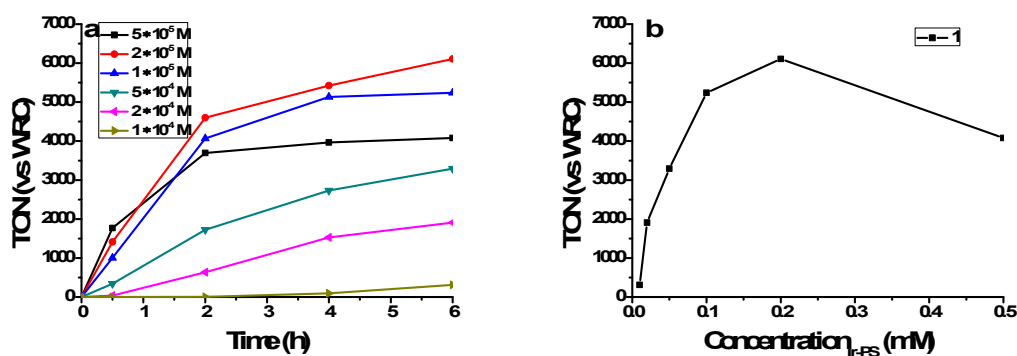


**Figure S7.** (a) Photocatalytic H<sub>2</sub> production profiles of the AP systems containing 1 μM **1**, 0.45 M TEA, and varied concentrations of [Ir(ppy)<sub>2</sub>(dtbbpy)]Cl in CH<sub>3</sub>CN/H<sub>2</sub>O (9:1); (b) H<sub>2</sub> production amounts of the AP systems after 6 h irradiation.

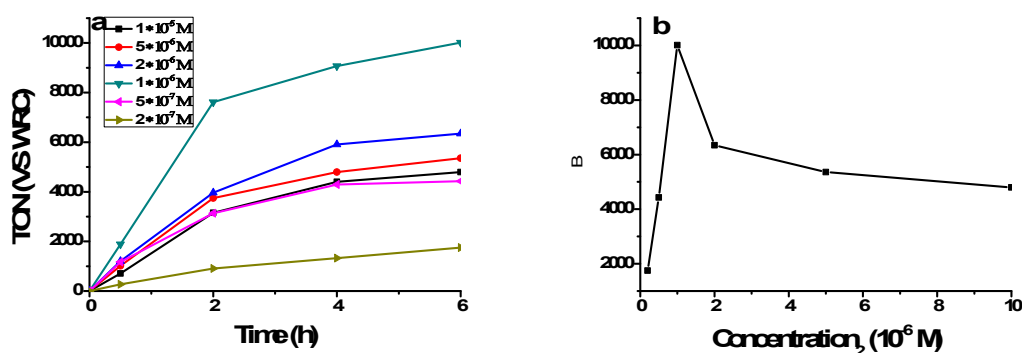


**Figure S8.** (a) Photocatalytic H<sub>2</sub> production profiles of the AP systems containing 0.2 mM [Ir(ppy)<sub>2</sub>(dtbbpy)]Cl, 0.45 M TEA, and varied concentrations of **2** in CH<sub>3</sub>CN/H<sub>2</sub>O (9:1). (b) H<sub>2</sub> production amounts of the AP systems after 5 h irradiation.

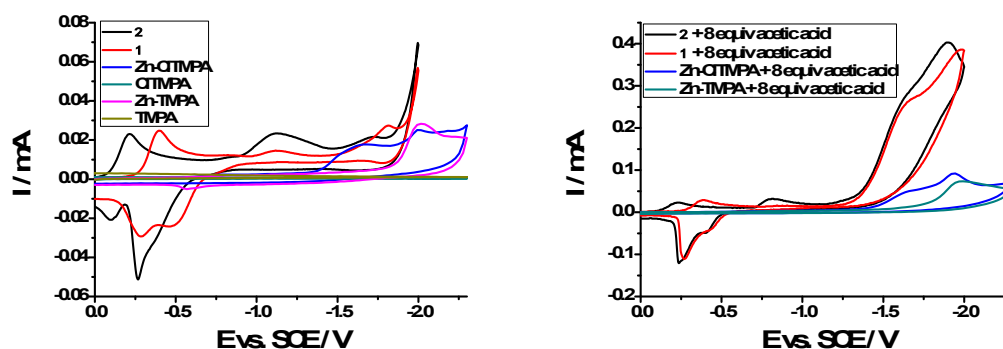


**Figure S9.** (a) Cyclic voltammograms of **1**, **2**, TMPA, Cl-TMPA, Zn-TMPA and Zn-Cl-TMPA (1 mM) in Ar-saturated CH<sub>3</sub>CN. Zn-TMPA and Zn-Cl-TMPA denote the in-situ formed Zn complexes of TMPA and Cl-TMPA by addition of excess Zn(BF<sub>4</sub>)<sub>2</sub> into the solutions. (b) Cyclic voltammograms of **1**, **2**, Zn-TMPA and Zn-Cl-TMPA (1 mM) in Ar-saturated CH<sub>3</sub>CN in the presence of 8 equivalent of acetic acid. Condition: 0.1 M *n*-Bu<sub>4</sub>NPF<sub>6</sub>, scan rate 100 mV/s.

For **1**, the -1.81 V peak may result from either Cu(I)/Cu(0) or TMPA/TMPA<sup>-</sup> or both. Therefore, we measured electrochemical properties of TMPA either free in solution or coordinated onto an

electrochemical inert metal center of  $\text{Zn}^{2+}$ .

TMPA ligand alone is electrochemical inert within the potential window of 0 ~ -2.0 V (vs. SCE), as shown in Figure S9a. Addition of  $\text{Zn}(\text{BF}_4)_2$  led to in-situ formation of the TMPA-based Zn complexes. In such a case, a redox process was observed with a peak at -2.0 V, which may be ascribed to the reduction of the TMPA ligands that have coordinated onto  $\text{Zn}^{2+}$  center. The peak profile also has a large difference with respect to **1** in the same potential window. More importantly, no electrocatalytic currents were found when acetic acid was added (Figure 9b), suggesting that  $\text{TMPA}^-$  alone or that has coordinated onto  $\text{Zn}^{2+}$  ion cannot lead to catalytic  $\text{H}_2$  evolution and Cu(I) should play an important role. Similar behaviors were also found for Cl-TMPA (Figure S9). Based on these facts and the proposed mechanism of the first Cu complex-based electrocatalytic WRC, the redox process for **1** at -1.81 V may be assigned to Cu(I)/Cu(0) or the mixture of Cu(I)/Cu(0) and TMPA/TMPA $^-$ .

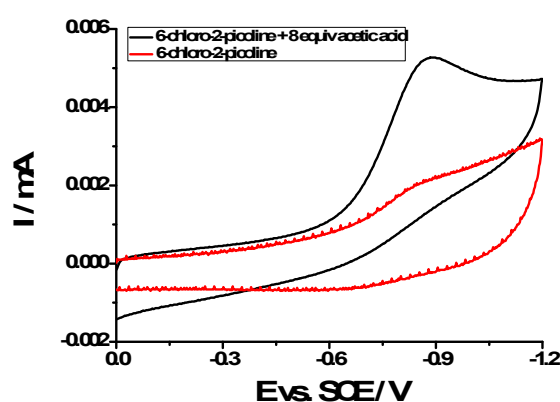


**Figure S10.** Cyclic voltammograms of 6-chloro-2-picoline (1 mM) in Ar-saturated  $\text{CH}_3\text{CN}$  with or without the presence of 8 equivalent acetic acid. Condition: 0.1 M  $n\text{-Bu}_4\text{NPF}_6$ , scan rate 100 mV/s.

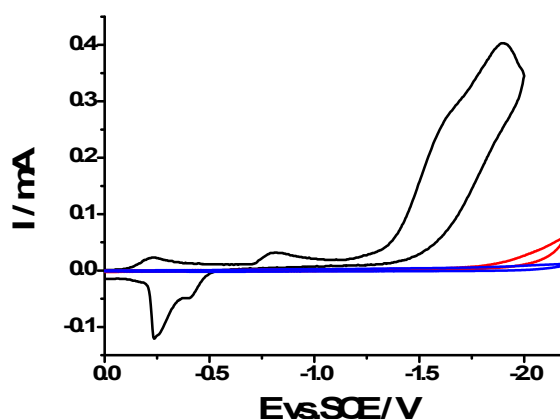


**Figure S11.** Cyclic voltammograms of blank  $\text{CH}_3\text{CN}$  (blue), 8 mM acetic acid in  $\text{CH}_3\text{CN}$  (red), and 8 mM acetic acid and 1 mM **2** in  $\text{CH}_3\text{CN}$  (black). Condition: 0.1 M  $n\text{-Bu}_4\text{NPF}_6$ , scan rate 100 mV/s.

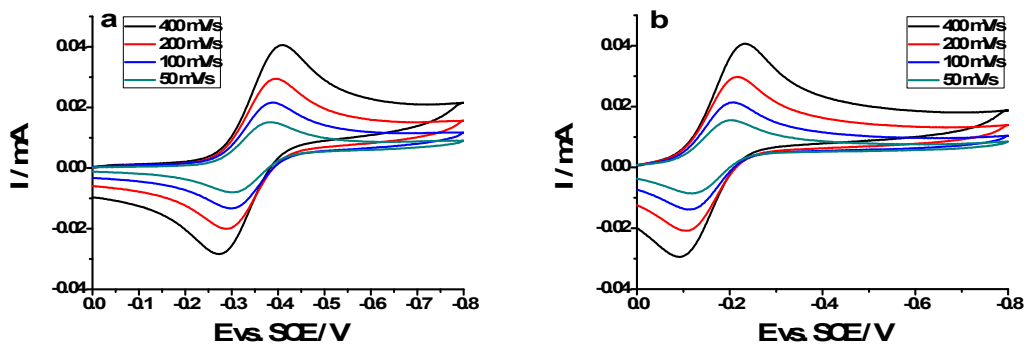


**Figure S12.** Cyclic voltammograms of 1 mM **1** (a) and **2** (b) in Ar-saturated CH<sub>3</sub>CN at different scan rates. Condition: 0.1 M *n*-Bu<sub>4</sub>NPF<sub>6</sub>.

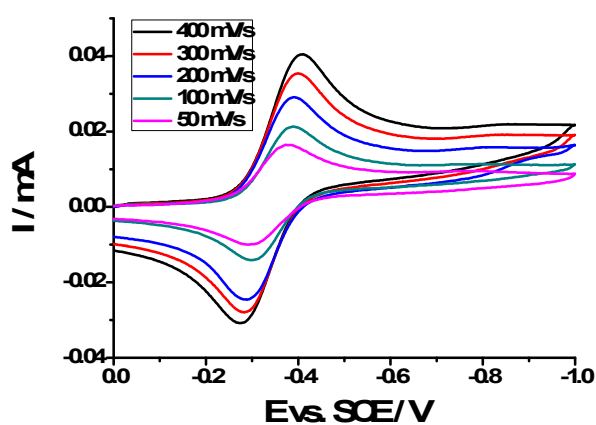


**Figure S13.** Cyclic voltammograms of **1** in Ar-saturated CH<sub>3</sub>CN at different scan rates. Condition: 0.1 M *n*-Bu<sub>4</sub>NPF<sub>6</sub>.

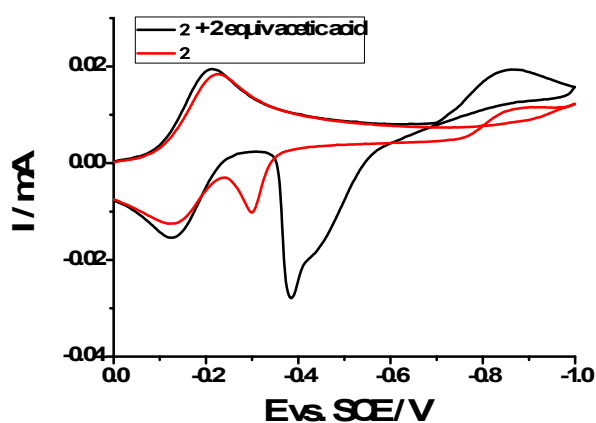


**Figure S14.** Cyclic voltammograms of **2** (1 mM) in Ar-saturated CH<sub>3</sub>CN with or without the presence of 2 mM acetic acid. Condition: 0.1 M *n*-Bu<sub>4</sub>NPF<sub>6</sub>, scan rate 100 mV/s.

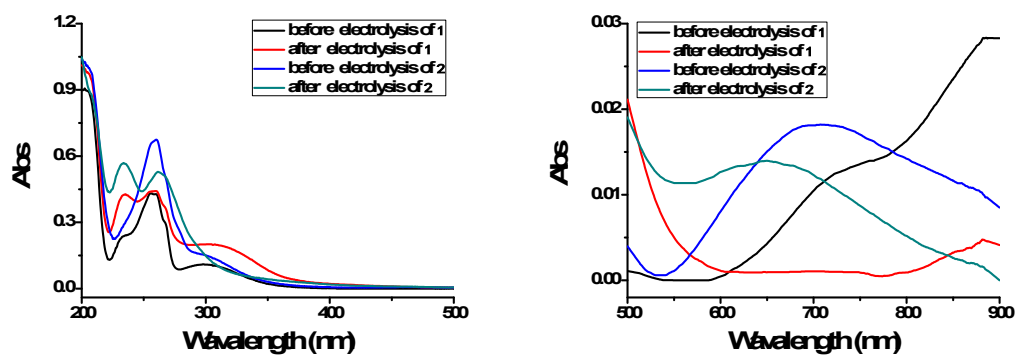


Figure S15. Absorption spectra of **1** and **2** before and after electrolysis at -1.8 V (vs. SCE) for 2 h.

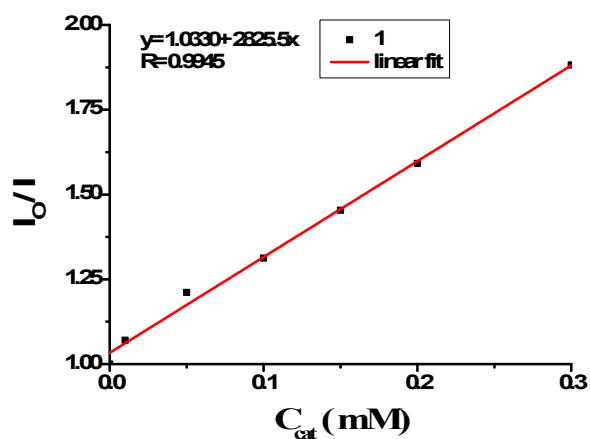


Figure S16. Stern-Volmer plot of the luminescence quenching of  $[\text{Ir}(\text{ppy})_2(\text{dtbp})]\text{Cl}$  by **1** in  $\text{CH}_3\text{CN}/\text{H}_2\text{O}$  (9:1).

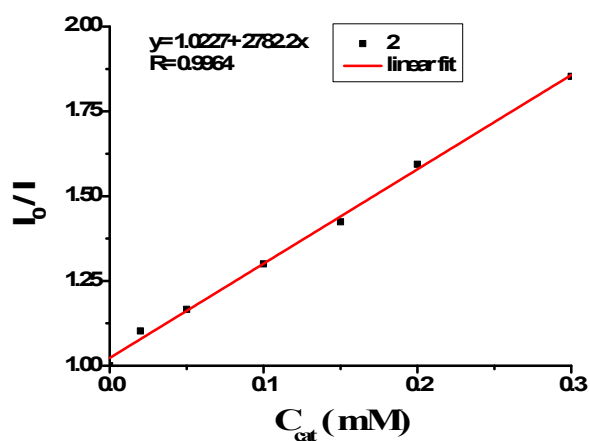
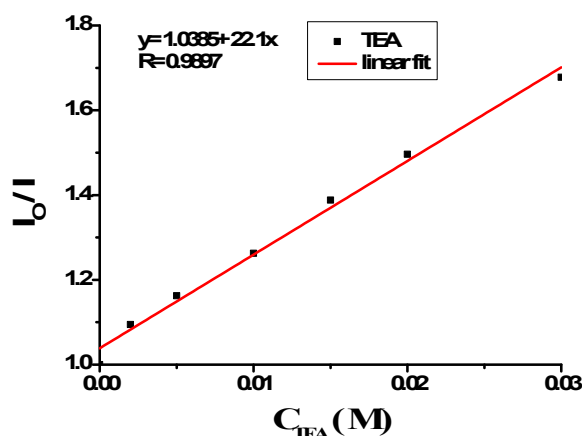


Figure S17. Stern-Volmer plot of the luminescence quenching of  $[\text{Ir}(\text{ppy})_2(\text{dtbp})]\text{Cl}$  by **2** in  $\text{CH}_3\text{CN}/\text{H}_2\text{O}$  (9:1).



**Figure S18.** Stern-Volmer plot of the luminescence quenching of  $[\text{Ir}(\text{ppy})_2(\text{dtbp})]\text{Cl}$  by TEA in  $\text{CH}_3\text{CN}/\text{H}_2\text{O}$  (9:1).

**Table S1.** Crystallographic data and processing parameters of **2**.

Complex	$[\text{Cu}(\text{Cl-TMPA})\text{Cl}_2]\text{Cl}$
Formula	$\text{C}_{18}\text{H}_{17}\text{Cl}_3\text{CuN}_4$
Formula weight	477.27
Temperature	293k
Wavelength	0.71073
Crystal system, space group	Monoclinic, $P2(1)/n$
Unit cell dimensions	$a = 7.513(2)$ Å $\alpha = 90$ deg $b = 32.062(8)$ Å $\beta = 111.229(3)$ deg. $c = 8.785(2)$ Å $\gamma = 90$ deg.
<i>Volume</i>	$1972.7(9)$ Å <sup>3</sup>
Z, Calculated density	4, 1.607 Mg/m <sup>3</sup>
Absorption coefficient	$1.530$ mm <sup>-1</sup>
F(000)	972
Crystal size	0.30 x 0.05 x 0.04 mm
Theta range for data collection	2.98 to 31.53 deg
Limiting indices	$-11 \leq h \leq 10$ , $-46 \leq k \leq 47$ , $-12 \leq l \leq 12$
Reflections collected / unique	27250 / 6537 [R(int) = 0.0536]
Completeness to theta = 31.53	99.6 %
Absorption correction	Semi-empirical from equivalents
Max. and min. transmission	0.9413 and 0.6568
Refinement method	Full-matrix least-squares on F <sup>2</sup>
Data / restraints / parameters	6537 / 3 / 253
Goodness-of-fit on F <sup>2</sup>	1
Final R indices [I > 2σ(I)]	R1 = 0.0554, wR2 = 0.1382
R indices (all data)	R1 = 0.0741, wR2 = 0.1517
Extinction coefficient	0.0010(7)
Largest diff. peak and hole	0.972 and -0.882 e.Å <sup>-3</sup>

**Table S2.** Selected bond lengths (Å) and angles (deg) of **2**.

Complex	[Cu(Cl-TMPA)Cl <sub>2</sub> ]Cl
Cu(1)-N(2)	2.011(2)
Cu(1)-N(3)	2.015(2)
Cu(1)-N(1)	2.063(2)
Cu(1)-Cl(3)	2.2533(8)
Cu(1)-Cl(2)	2.5751(9)
N(2)-Cu(1)-N(3)	160.90(9)
N(2)-Cu(1)-N(1)	80.28(9)
N(3)-Cu(1)-N(1)	81.67(9)
N(2)-Cu(1)-Cl(3)	97.37(7)
N(3)-Cu(1)-Cl(3)	97.69(7)
N(1)-Cu(1)-Cl(3)	161.12(7)
N(2)-Cu(1)-Cl(2)	93.47(7)
N(3)-Cu(1)-Cl(2)	94.55(7)
N(1)-Cu(1)-Cl(2)	95.88(7)
Cl(3)-Cu(1)-Cl(2)	102.97(3)

### References

1. F. De Angelis, S. Fantacci, N. Evans, C. Klein, S. M. Zakeeruddin, Jacques-E. Moser, K. Kalyanasundaram, H. J. Bolink, M. Graetzel and M. K. Nazeeruddin, *Inorg. Chem.*, 2007, **46**, 5989-6001.
2. (a) S. Kim, C. Saracini, M. A. Siegler, N. Driehko and K. D. Karlin, *Inorg. Chem.*, 2012, **51**, 12603-12605; (b) D. Maiti, A. A. N. Sarjeant and K. D. Karlin, *J. Am. Chem. Soc.*, 2007, **129**, 6720-6721.
3. P. Zhang, M. Wang, Y. Yang, T. Yao, and L. Sun, *Angew. Chem. Int. Ed.*, 2014, **53**, 13803-13807.
4. A. Nanthakumar, S. Fox, N. N. Murthy and K. D. Karlin, *J. Am. Chem. Soc.*, 1997, **119**, 3898-3906.